Parametric Study on Shape Dependence of Inductively Coupled Plasma Cathode for Performance Improvement

IEPC-2011-305

Presented at the 32nd International Electric Propulsion Conference,
Wiesbaden • Germany
September 11 – 15, 2011

Takuya Nakabayashi[1] Hiroki Watanabe[2] Satoshi Kasagami[3] Junichiro Aoyagi[4] and Haruki Takegahara[5]
Department of Aerospace Engineering, Tokyo Metropolitan University, Hino, Tokyo, 191-0065, Japan

Abstract: The inductively coupled plasma cathode has been developed as electron source for ion thruster. The power consumption efficiency of this cathode was not sufficient for practical use in space. Therefore, in order to improve the cathode performance, the effects of orifice diameter, orifice length, ion collector shape and coil configuration on ignition capability and electron emission performance were investigated experimentally in this study. As a result, it is also estimated that inner pressure and electric field in the vessel affect ignition capability. Moreover, electron emission performance depends on inner pressure, ion collection area and electron number density. In addition, the increase of total number of coils improves ignition capability and electron emission performance. Through the performance improvement, 0.52 A of anode current was obtained at 24 W of plasma production power, 0.15 mg/s of xenon mass flow rate and 40 V of anode voltage.

Nomenclature

A_i	=	ion collection area
A_o	=	orifice cross section area
C_e	=	electron production cost
e	=	electron charge
F	=	gas utilization factor
F_o	=	orifice conductance
F_{fm}	=	free-molecular conductance
F_{fm0}	=	theoretical free-molecular conductance
I_a	=	anode current
I_c	=	collector current
I_{is}	=	ion saturation current at ion collector
I_{rf}	=	peak radio frequency current
J_{is}	=	ion saturation current density
j	=	imaginary unit
K	=	Clausing's factor
Kn	=	Knudsen number
k	=	Boltzmann coefficient
M	=	molecular mass
m_i	=	ion mass

[1] Graduate Student, Department of Aerospace Engineering, t-nakabayashi@astak3.sd.tmu.ac.jp.
[2] Graduate Student, Department of Aerospace Engineering, hwatanabe@astak3.sd.tmu.ac.jp.
[3] Graduate Student, Department of Aerospace Engineering, s-kasagami@astak3.sd.tmu.ac.jp.
[4] Assistant Professor, Department of Aerospace Engineering, j-aoyagi@astak3.sd.tmu.ac.jp.
[5] Professor, Department of Aerospace Engineering, hal@astak3.sd.tmu.ac.jp.

$\dot{m}$ = mass flow rate
N_A = Avogadro constant
N_e = electron number density in the bulk plasma
N_i = ion number density in the bulk plasma
P_a = anode power for electron extraction
P_{abs} = absorbed power into plasma
P_{loss} = power loss in induction coil
P_{rf} = radio frequency power
p_{in} = vessel inner pressure
p_0 = backpressure in vacuum chamber
Q = flow rate
R = cathode resistance without plasma
T_e = electron temperature
T_n = gas temperature
V_a = anode voltage
V_{rf} = peak radio frequency voltage
v_a = mean molecular velocity
X = cathode reactance without plasma
Z = cathode impedance without plasma
$|Z|$ = absolute value of impedance
η = power transfer efficiency
θ = phase shift between radio frequency current and voltage
ν_e = electron collision frequency

I. Introduction

THE applications of electric propulsion have been increasing in some space missions such as station keeping and solar system exploration. An ion thruster is one of the electric propulsion systems, which has the highest specific impulse and thrust efficiency but low thrust[1]. Therefore, the thruster requires long continuous operation to generate large total impulse. The lifetime of ion thruster is limited by acceleration electrodes and electron sources. Ion thruster needs electron sources as a discharge cathode for ionization of propellant and a neutralizer for neutralization of ion beam. A hollow cathode (H/C) is a common electron source for DC discharge and radio frequency (RF) discharge ion thrusters, because it achieves high electron emission current with low consumption of gas and electric power. However, its lifetime is limited by degradation and depletion of a thermionic emitter made from low work function materials[2,3]. Additionally, the emitter has to avoid the contact with active gas and the cathode requires sufficient preheating by heater wire before ignition. As a result, ion thrusters with H/C have some difficulties for long term operation, and they should be controlled strictly from prelaunch to end of life.

In order to replace the hollow cathode as the electron source, new cathodes, which employ RF discharge or microwave discharge for electron production, have been developed[4-7]. The microwave discharge ion thruster "μ10", which was installed in "Hayabusa" asteroid explorer, is attractive thruster that is hollow-cathode-less design. Its accumulated operational time reached 35,000 hours and the thruster demonstrated that the removal of the hollow cathode benefits the lifetime of ion thruster[8]. However, since electron cyclotron resonance plasma (ECRP) is applied, the electron number density is limited by cutoff frequency and the plasma of ion source is not uniform. Additionally, a microwave generator is low power efficiency that is below 50 %. Consequently, thrust performance of microwave discharge ion thrusters is lower than that of other discharge type ion thrusters.

We have proposed employing inductively coupled plasma (ICP) as electron sources for ion thrusters. ICP cathode (herein after referred to "ICP/C") is simple structure, which does not need a keeper electrode and a bias power supply to emit electrons. Additionally, ICP/C is excepted long lifetime because it does not use chemical reaction such as the thermionic emitter of H/C. Moreover, the ignition sequence of ICP/C is simplicity and strict thermal control is not required.

In our previous study, it was demonstrated that the ICP/C operated as electron sources of ion thrusters[9]. When ICP/C or H/C applied to the discharge cathode of DC ring-cusp ion thruster, same values of thrust and specific impulse were obtained at each cathode with equal propellant consumption. However, the power consumption of ICP/C is higher than that of H/C to achieve equivalent discharge current. Therefore, thrust-to-power ratio and ion production cost with ICP/C were inferior to those with H/C.

II. Objective

Based on the previous results, in order to improve ICP/C performance, its ignition capability and electron emission performance were investigated experimentally in this study. The effect of orifice diameter, orifice length, ion collector shape and coil configuration were evaluated and discussed.

III. Experimental Apparatus and Procedure

A. Inductively Coupled Plasma Cathode

Figure 1 shows the schematic diagram of ICP/C. It consists of discharge vessel, ion collector, induction coil and housings. The vessel is made of alumina, its inner diameter and length are 40 mm and 25 mm, respectively. For electron emission, there is an orifice at the center of the end of vessel. The molybdenum electrode is inserted into the vessel as an ion collector. When electrons are emitted from orifice, ions that are equal to them must be collected at the collector to maintain quasineutrality at ICP. In addition, the copper wire was wrapped around the vessel to introduce RF power. Features of the cathode are simple structure and thermionic-emitter-less design.

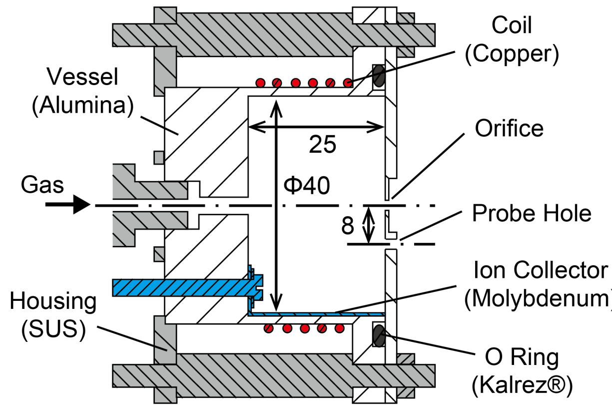

Figure 1. Schematic diagram of ICP/C.

In this study, collector shape, orifice diameter, orifice length and coil configuration were varied. The effects of three ion collector shapes including no ion collector were investigated, when the orifice diameter, the orifice length and the number of coils were 2.0 mm, 0.5 mm and 5 turns, respectively. Figure 2 shows two types of ion collector, which are cylindrical type and pole type, where A_i is the ion collection area. The cylindrical collector has an axial slit, which allows the axial dB/dt fields into plasma but suppresses the circumferential dE/dt fields, effectively serving as a Faraday shield for the plasma within ICP/C[10]. On the other hand, in order to investigate the relationship between the ion collection area and the electron emission performance, the area of pole collector is set up larger than that of cylindrical one.

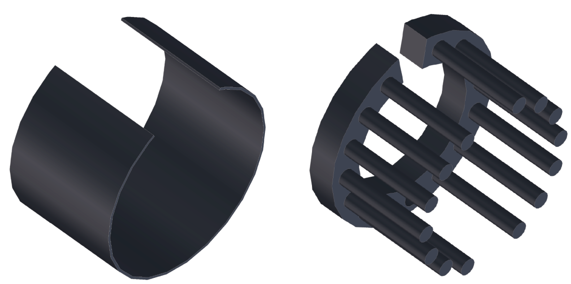

Figure 2. Ion collector shape.

The orifice configurations were varied five patterns to investigate the effects of orifice dimensions, when the ion collector shape was the cylindrical and the number of coils was 5 turns. Table 1 shows these patterns and the notation system. "D2-L0.5" in Table 1 indicates the orifice diameter and the orifice length are 2.0 mm and 0.5 mm, respectively.

Table 1. Orifice dimension.

Diameter	Length		
	0.5 mm	1.0 mm	2.0 mm
1.0 mm	D1-L0.5		
2.0 mm	D2-L0.5	D2-L1	D2-L2
3.0 mm	D3-L0.5		

The number of coils was varied from 3 turns to 6 turns to investigate the effects of coil configuration, when orifice diameter, orifice length and ion collector are 2.0 mm, 0.5 mm and cylindrical collector, respectively. The coil pitch was constant when the number of coils was varied.

B. Apparatus and Facilities

Figure 3 shows the experimental setup. All experiments were conducted in the vacuum chamber whose diameter and length are 1.6 m and 3.2 m, respectively. Backpressure in the chamber reached approximately 2×10^{-3} Pa, when xenon mass flow rate was 0.6 mg/s. The ICP/C, an anode electrode and a double probe were set in the chamber, whereas RF transmission system, gas feed system and DC power supplies were attached from outside of the chamber. Xenon was fed to the vessel via mass flow controller (MFC) as operation gas. The coil was energized at 13.56 MHz with the RF generator via resonant matching circuit, which consists of a series variable capacitor and a parallel variable capacitor. Since the impedance of generator was matched that of the ICP/C by the circuit, there was not reflected RF power at all experiments. The anode was located at 50 mm downstream of the ICP/C, and it was biased positively to extract electrons from ICP/C. On the other hand, ion collector was connected to ground potential. The electric potential difference between the anode and the grounded ion collector simulates the difference between the ion beam and the neutralizer. When electrons are emitted from the ICP/C by the difference of the potential, electron current is carried to the anode and ion current is carried to the collector. These currents were called anode current and collector current, respectively. The anode current is equal to the collector current (I_a=I_c) because the current loop must close in this experimental system to evaluate performance. The amount of anode current at constant RF power and xenon mass flow rate indicates the electron emission performance of electron sources. Additionally, in order to measure plasma parameter, the double probe was inserted into the vessel[11-13].

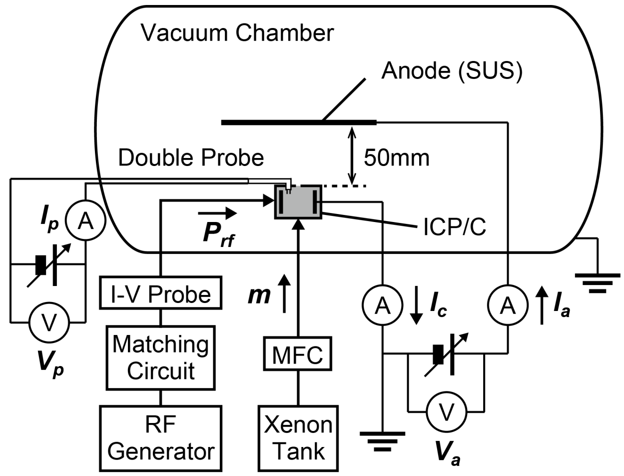

Figure 3. Experimental Setup.

C. Calculation of Cathode Impedance and Vessel Inner Pressure

Before measuring the ignition capability, cathode impedance and vessel inner pressure were calculated in order to estimate experimental condition of various cathode configurations. When RF power was below 40 W, The characteristics of RF current and RF voltage without plasma were measured to calculate an impedance of ICP/C. The impedance is given by

$$|Z| = \frac{V_{rf}}{I_{rf}} \tag{1}$$

$$\theta = \cos^{-1}\frac{2P_{rf}}{V_{rf}I_{rf}} \tag{2}$$

$$Z = |Z|\left(\cos\theta + j\sin\theta\right) = R + jX \tag{3}$$

where I_{rf}, V_{rf}, θ, R and X are peak RF current, peak RF voltage, phase shift between RF current and voltage, cathode resistance and cathode reactance without plasma, respectively. When RF power was higher than 40 W, RF voltage between the coil ends was calculated by following equation because of maximum input voltage in the voltage probe.

$$V_{rf} = \sqrt{\frac{2|Z|P_{rf}}{\cos\theta}} \tag{4}$$

On the other hand, vessel inner pressure was not measured but calculated. The pressure was calculated by a conductance of short circular tube at rarefied flow[14,15]. The orifice conductance F_o in the ICP/C is given by

$$\begin{aligned} F_o &= \frac{0.4733 + A\sqrt{1/(a/Kn)}}{1 + B/(a/Kn) + C/(a/Kn)^2} F_{fm0} + F_{fm} \\ a &= \frac{F_{fm}}{F_{fm0}} + 0.125\exp\left[-\frac{1}{2}\left(12\frac{F_{fm}}{F_{fm0}} - 11.2\right)^2\right] + 0.18\exp\left(-14.7\frac{F_{fm}}{F_{fm0}}\right) - 0.08, \\ A &= 0.907, B = 10.4, C = 16.1 \end{aligned} \tag{5}$$

where Kn, F_{fm0} and F_{fm} are Knudsen number, theoretical free-molecular conductance and free-molecular conductance, respectively. These conductance are given by

$$F_{fm0} = \frac{1}{4} v_a A_o = \frac{1}{4} \sqrt{\frac{8kN_A T_n}{\pi M}} A_o \tag{6}$$

$$F_{fm} = KF_{fm0} \tag{7}$$

where v_a, T_n, M, A_0, and K are mean molecular velocity, gas temperature, molecular mass, orifice cross section area and Clausing's factor which depends on orifice diameter and length, respectively. Equation (5) is empirical equation, even though the range of applicability is restricted to $1/K_n < 25$. Using calculated orifice conductance by Eq. (5), vessel inner pressure is given by

$$p_{in} = \frac{Q}{F_o} + p_o \tag{8}$$

where p_{in}, p_0 and Q are vessel inner pressure, backpressure in the vacuum chamber and xenon flow rate which is provided at standard temperature and pressure, respectively. In this study, the backpressure was ignored because it was much lower than the inner pressure.

IV. Results and Discussions

A. Calculation Results of Resistance and Reactance

Table 2 shows the calculated resistance and reactance of ICP/C without plasma at various cathode configurations. The resistance and reactance were calculated by RF voltage and RF current in Eqs. (1)-(3), when the power loss and the stray impedance are ignored at the matching circuit and transmission lines. In Table 2, it is considered that the resistance and reactance were independent of orifice dimensions because the values did not change when orifice dimension was varied. On the other hand, they depended on ion collector and coil configurations. The reactance without ion collector was higher than that with ion collector. It is assumed that a capacitive coupling between the energized coil and the grounded collector is the cause to increase the reactance. The reactance increased approximately with the square of total number of coils.

The RF voltage between coil ends was also independent of the orifice dimensions because the voltage has a relationship with the impedance as shown in Eq. (4). On the other hand, the voltage also depended on collector and coil configurations, and it increased with collector insertion and increase of total number of coils at constant RF power.

Table 2. Calculated resistance and reactance of ICP/C without plasma at various cathode configurations.

Orifice diameter	Orifice length	Collector configuration	Total number of coils	Resistance	Reactance
1.0 mm	0.5 mm	Cylindrical	5 turns	2.5±0.1 Ω	103±1 Ω
2.0 mm	**0.5 mm**	**Cylindrical**	**5 turns**	2.6±0.1 Ω	102±1 Ω
3.0 mm	0.5 mm	Cylindrical	5 turns	2.7±0.2 Ω	102±1 Ω
2.0 mm	**1.0 mm**	Cylindrical	5 turns	2.7±0.1 Ω	103±1 Ω
2.0 mm	**2.0 mm**	Cylindrical	5 turns	2.6±0.1 Ω	102±1 Ω
2.0 mm	0.5 mm	**without**	5 turns	1.9±0.1 Ω	111±1 Ω
2.0 mm	0.5 mm	**Pole**	5 turns	2.1±0.1 Ω	103±1 Ω
2.0 mm	0.5 mm	Cylindrical	**3 turns**	1.8±0.1 Ω	50±1 Ω
2.0 mm	0.5 mm	Cylindrical	**4 turns**	2.1±0.1 Ω	76±1 Ω
2.0 mm	0.5 mm	Cylindrical	**6 turns**	3.8±0.1 Ω	137±1 Ω

B. Ignition Capability

1. Effects of cathode configurations on ignition capability

Figure 4 shows ignition capability of ICP/C when cathode configurations were varied. It is preferable that the plasma is ignited at low RF power and mass flow rate. Thus, points on the graph go to left below equal to improve ignition capability in Fig. 4. In addition, red circle means same result when the configuration is 2.0 mm of orifice diameter, 0.5 mm of orifice length, cylindrical type of ion collector shape and 5 turns of coil turns.

Figure. 4(a) and (b) indicates that orifice diameter strongly affected the capability rather than orifice length. Additionally, the ignition capability was enhanced with decreasing orifice diameter and increasing orifice length. In Fig. 4(c), higher RF power is necessary for ignition with ion collector, compared with "without ion collector". This indicates that the ion collector causes change of electric field. Regarding the ignition capability, the cylindrical collector was preferable to the pole collector. In addition, it became clear that the collector shape affects the capability greatly. Moreover, the ignition capability was enhanced with increasing total number of coils as shown in Fig. 4(d). However, enhancement rate is decreased as increasing total number of coils. It would appear that there exists saturation number, which enhance ignition capability. In Fig. 4, regardless of cathode configurations, a steep decrease of minimum ignition RF power was observed as xenon mass flow rate increased, and there was a knee point between power and mass flow rate for plasma ignition of ICP/C. It seems that plasma ignition of ICP/C is involved in Paschen's law[16].

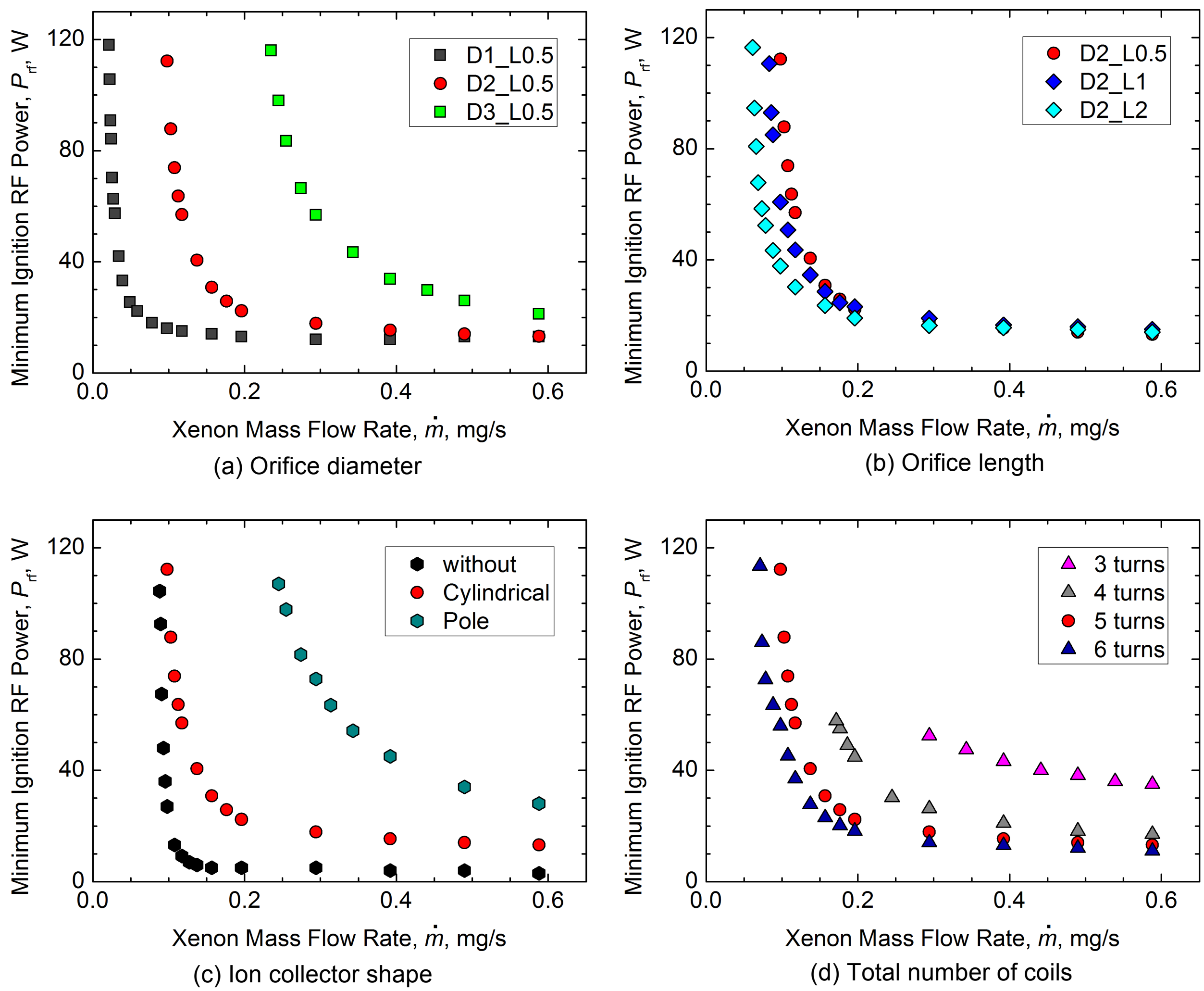

Figure 4. Effects of cathode configuration on ignition capability.

2. Factors of plasma ignition in ICP/C

Plasma ignition of ICP/C is thought the trade-off study between voltage and inner pressure. Minimum ignition RF voltage as a function of inner pressure at various cathode configurations is shown in Fig. 5. In this figure, the voltage and the pressure were not measured but calculated as described above. The voltage was calculated by measured minimum ignition RF power in Eq. (4), while the pressure was calculated by orifice dimensions and fed xenon mass flow rate in Eqs. (5)-(8). In Fig. 5(a) and 5(c), the curves of voltage vs. pressure nearly corresponded with one another. Therefore, it is considered that the plasma ignition is affected by inner pressure in the discharge vessel and RF voltage between the coil ends. On the other hand, the curves did not correspond with one another as shown in Fig. 6(b). It is assumed that electric field in the vessel was changed by the collector shape. In contrast with the effect of coil configuration, the collector configuration affected the electric field at constant RF voltage, because the collector was made of metal and connected to ground potential. Thus, the difference of electric field in the vessel caused the distinct tendency in Fig. 5(b).

As a result, it is considered that inner pressure and electric field in the discharge vessel are the plasma ignition factors in ICP/C.

C. Electron Emission Performance

1. Effects of cathode configuration on electron emission performance

Figure 6 shows the effect of cathode configuration on electron emission performance of ICP/C when xenon mass flow rate and anode voltage was 0.15 mg/s and 40 V, respectively. The anode current was proportional to RF power regardless of cathode configuration. There existed the difference in the inclination by change cathode configuration.

Figure. 6(a) and (b) show that the orifice diameter strongly affected electron emission performance rather than orifice length. The data presented in Fig. 6(c) shows that electrons cannot be emitted from the cathode effectively without ion collector, because there is no counterpart to emit electron. In comparison of two ion collectors, pole collector was better than cylindrical one for electron emission performance at ICP/C. When the pole collector was inserted in the cathode, the typical performance was 0.52 A of the anode current at 24 W of RF power, 0.15 mg/s of xenon mass flow rate and 40 V of anode voltage. The value of anode current is high enough to neutralize the ion beam of ion thrusters, which have been employed for north south station keeping missions[17]. In Fig. 6(d), the performance was enhanced as total number of coils increases.

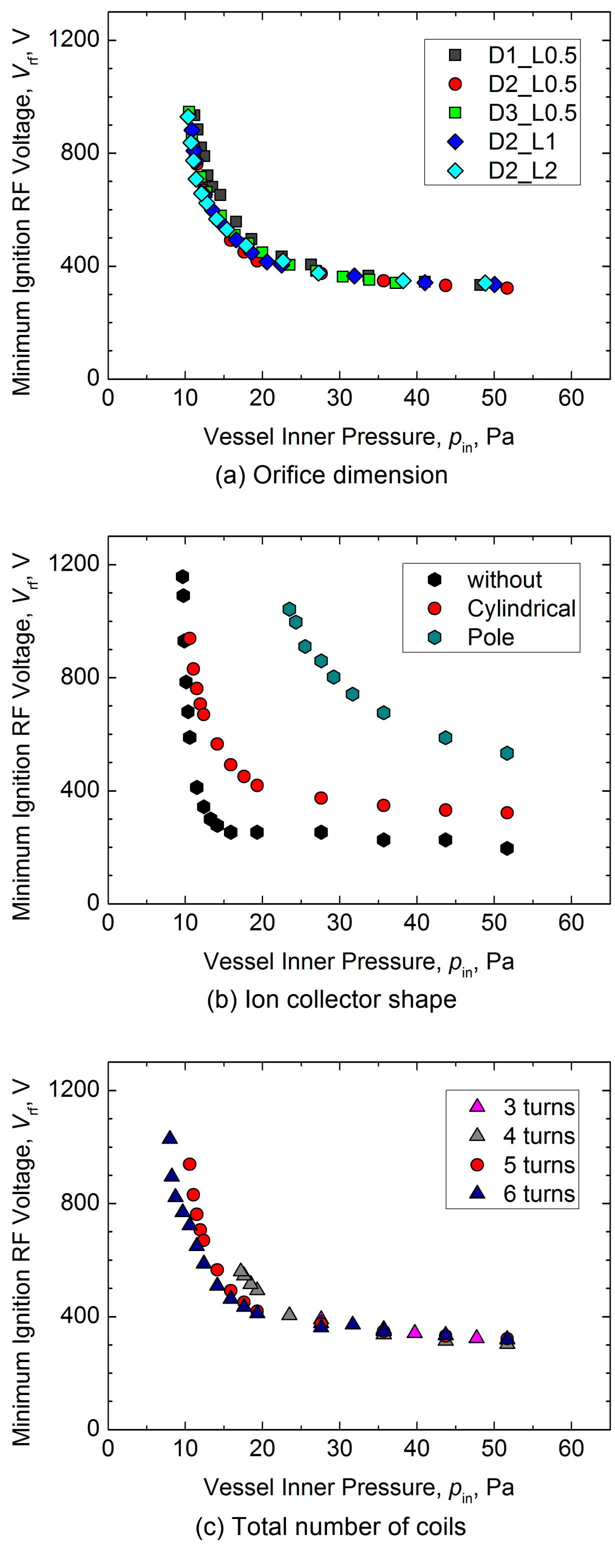

Figure 5. Minimum ignition RF voltage as a function of vessel inner pressure at various cathode configuration.

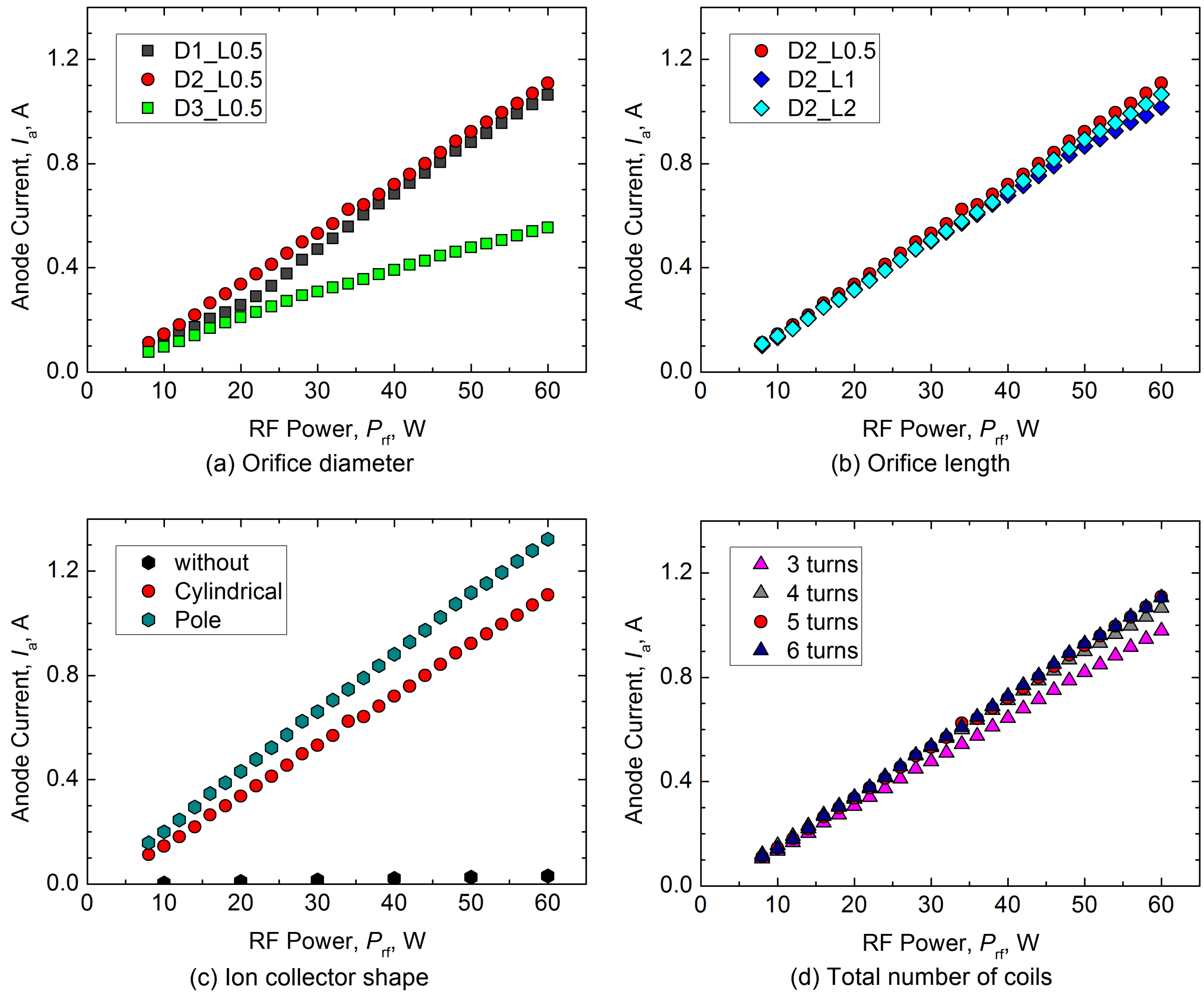

Figure 6. Effects of cathode configuration on electron emission performance at 0.15 mg/s of mass flow rate and 40 V of anode voltage.

2. Factors of limiting electron emission performance

From previous study, it became clear that the anode current saturates as anode voltage increases[9]. Figure 7 shows typical current-voltage characteristic of ICP/C, when RF power and mass flow rate are 40 W and 0.15 mg/s, respectively. The saturation of anode current occurred over 30 V of anode voltage, except for 3.0 mm of orifice diameter. Thus, anode current shown in Fig. 6 means maximum anode current at constant RF power and constant xenon mass flow rate.

In order to maintain quasineutrality at ICP/C, the amount of emitted electron from ICP/C have to be balanced by an equal amount of collected ion at the ion collector. When ions are collected by the collector, ion sheath is formed on its surface. An ion saturation current in collisionless ion sheath at low ion temperature is given by

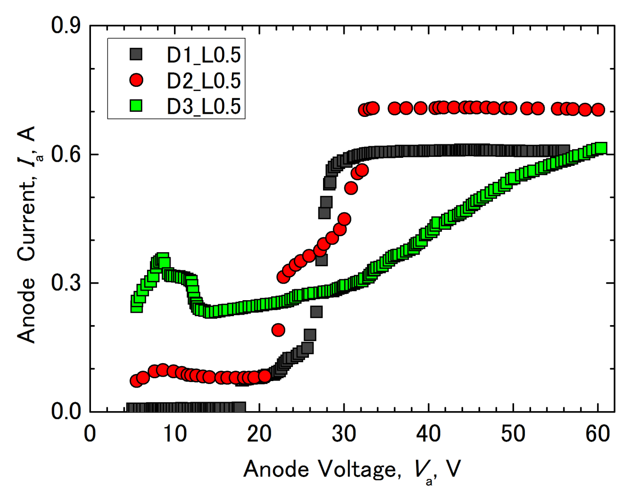

Figure 7. Typical current-voltage characteristic of ICP/C when varied the orifice diameter at 40 W of RF power and 0.15 mg/s of mass flow rate.

$$I_{is} = A_i J_{is} = A_i \alpha_i N_i e \sqrt{\frac{T_e}{m_i}} \tag{9}$$

where J_{is}, A_i, N_i, $\alpha_i N_i$, T_e and m_i are ion saturation current density, ion collection area in the collector, the ion number density in the bulk plasma, the ion number density at the sheath boundary, electron temperature and ion mass, respectively[18]. Generally the ion number density is presumed to be equal to electron number density in bulk plasma. Figure 8 shows ion saturation current, electron temperature and electron number density as a function of RF power, when the orifice diameter and length are 2.0 mm and 0.5 mm, respectively. The data of ion saturation current was collected by the double probe. In Fig. 8, the electron number density is proportional to RF power, whereas the electron temperature is independent of the power. If ion collection area and coefficient are constant, ion saturation current is proportional to the ion number density in Eq. (9). In fact, the ion saturation current is proportional to RF power as shown in Fig. 8. Because of the proportional relationship between anode current and RF power as shown in Fig. 6, it is considered that anode current is limited by collector current depending on the ion saturation current.

Figure 9 shows the effect of orifice diameter on anode current and plasma parameters at 20 W of RF power and 0.15 mg/s of xenon mass flow rate. The data in Fig. 9 shows electron number density decreased as the diameter increased. Therefore, the electron number density is highest of all diameters when the diameter is 1.0 mm. However, the maximum anode current was obtained at 2.0 mm of diameter. Thus, the orifice diameter of ICP/C has optimum value around 2.0 mm.

Figure 10 shows anode current, electron collision

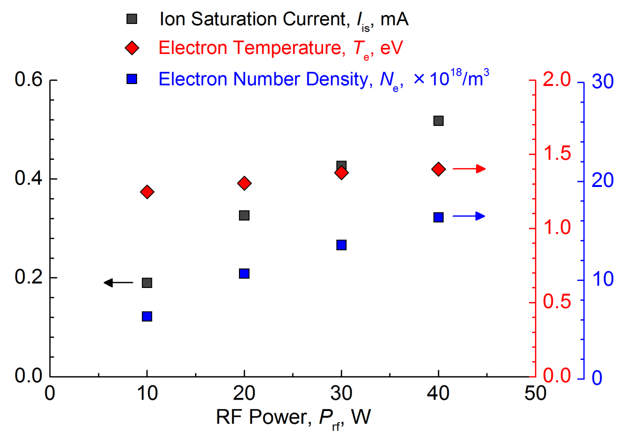

Figure 8. Typical ion saturation current, electron number density and electron temperature as a function of RF power.

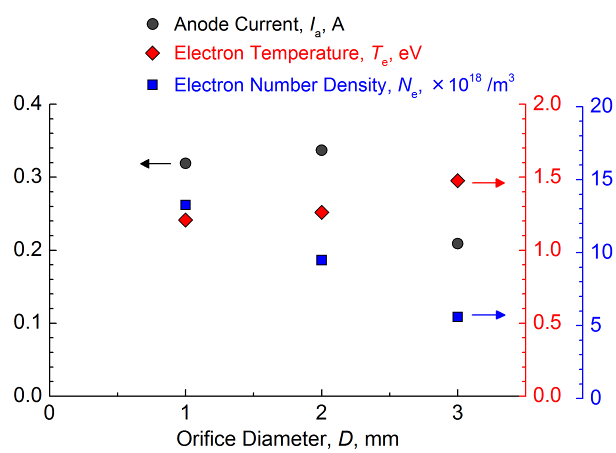

Figure 9. Effect of orifice diameter on anode current and plasma parameters at 20 W of RF power and 0.15 mg/s of xenon mass flow rate.

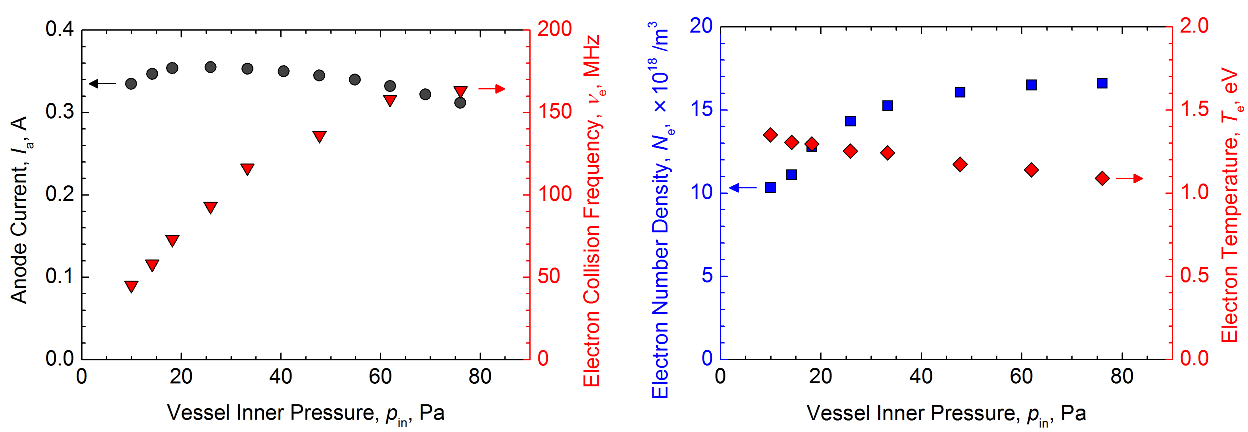

(a) Anode current and electron collision frequency

(b) Plasma parameters

Figure 10. Anode current, electron collision frequency and plasma parameters as a function of vessel inner pressure at 20 W of RF power and 2.0 mm of orifice diameter.

frequency and plasma parameters as a function of vessel inner pressure at 20 W of RF power and 2.0 mm of orifice diameter. The date in Fig. 10(a) shows that there existed optimum inner pressure for electron emission as the orifice diameter in Fig. 9. On the other hand, the electron number density increased as the vessel inner pressure increased as shown in Fig. 10(b). Therefore, it would appear that $\alpha_i N_i$ in Eq. (9) peaked at optimum pressure, which is approximately 25 Pa in Fig. 10(a). In addition, the electron collision frequency was nearly equal to driven angular frequency of 85.2 MHz when the anode current was maximized at 25 Pa of inner pressure.

Anode current with the pole collector was larger than that with the cylindrical collector at constant RF power and xenon mass flow rate as shown in Fig. 6(c). Figure 11 shows anode current ratio and saturation current density ratio of pole collector to cylindrical collector as a function of RF power at 0.15 mg/s of mass flow rate. In Fig. 11, the current density ratio was calculated when the coefficient α_i with the pole collector is equal to that with the cylindrical collector. The ratio was nearly equal to 1.0. Therefore, same plasma was produced at each collector, and ion saturation current density was presumed to be equal to the other. On the other hand, the anode current ratio is approximately equal to the ion collection area ratio of the pole collector to the cylindrical collector, which is 1.3 regardless of RF power. Consequently the amount of anode current strongly depends on ion collection area compared with ion collector shape.

As a result, it is considered that the anode current limited by collector current depending on the ion saturation current. Additionally, the ion saturation current strongly depends on vessel inner pressure, ion collection area and electron number density.

3. *Effects of total number of coils*

Figure 12 shows the effects of total number of coils on electron emission performance at 20 W of RF power and 0.15 mg/s of xenon mass flow rate. Power transfer efficiency η is given by

$$\eta = \frac{P_{abs}}{P_{rf}} = \frac{P_{rf} - P_{loss}}{P_{rf}} = \frac{P_{rf} - \frac{1}{2} I_{rf}^2 R}{P_{rf}} \tag{10}$$

where P_{abs},, P_{loss} and R are absorbed power into plasma, power loss in the induction coil and coil resistance, respectively[19,20]. The resistance is equal to the cathode resistance without plasma. The cathode resistance and reactance without plasma increased as total number of coils increased as shown in Table 2, and peak RF current decreased as the reactance increased. Therefore, the power loss in the coil decreased as total number of coils increased, because the loss depends on the resistance and the square of the RF current as shown in Eq. (10). The transfer efficiency rises due to the power loss decrease. Consequently, anode current increased as total number of coils increased as shown in Fig. 12. The minimum anode voltage, which is the lowest voltage for saturation of anode current, dropped as the number increased. Decrease of the minimum anode voltage is desirable for ICP/C lifetime, because ion sputtering yield against the molybdenum collector decreases. Therefore, total number of coils increases as large as possible not only for electron emission performance but also for lifetime.

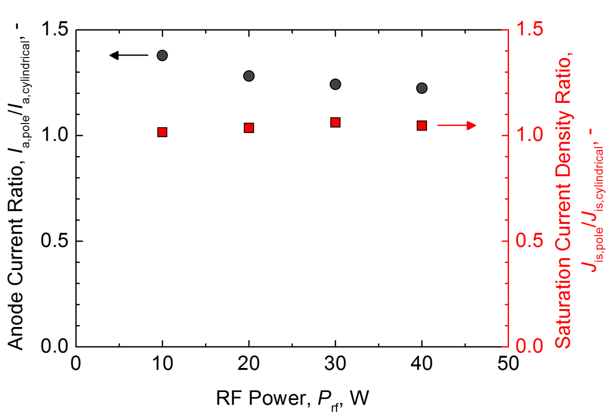

Figure 11. Anode current ratio and saturation current densitisy ratio of pole collector to cylindrical collector as a function RF power.

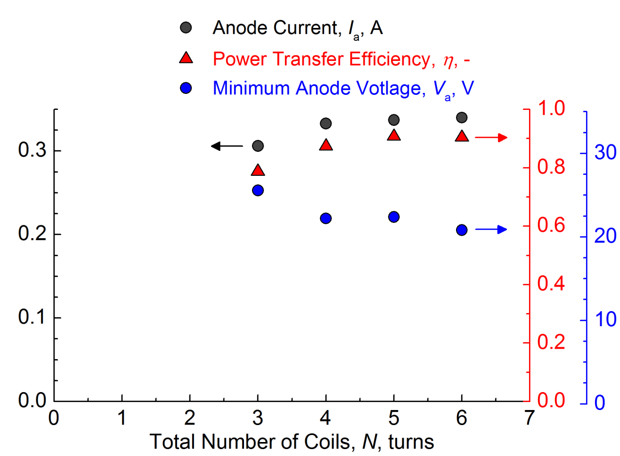

Figure 12. Effect of total number of coils on electron emission performance at 20 W of RF power and 0.15 mg/s of mass flow rate.

4. Performance of ICP/C in the present state

Figure 13 shows the relations among gas utilization factor and electron production cost at 0.15 mg/s of mass flow rate and 40 V of anode voltage. Electron production cost and gas utilization factor are given by

$$C_e = \frac{P_{rf} + P_a}{I_a} = \frac{P_{rf} + V_a I_a}{I_a} = \frac{P_{rf}}{I_a} + V_a \quad (11)$$

$$F = \frac{I_a}{0.718 \times \dot{m}} \quad (12)$$

where P_{rf}, P_a, I_a, V_a and $\dot{m}$ are RF power, anode power, anode current, anode voltage and mass flow rate, respectively. The gas utilization factor increases as rise of RF power. On the other hand, the electron production cost is approximately constant when RF power is changed. In Eq. (11), the second term is constant and the first term is proportional relation as shown in Fig. 6. Therefore, the gas utilization factor is increased at constant electron production cost by rise of RF power at ICP/C.

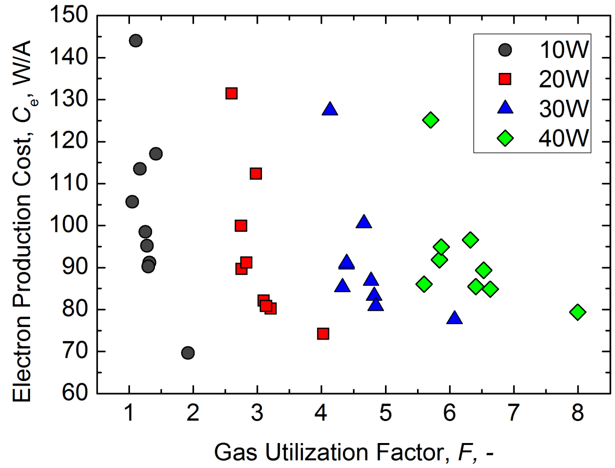

Figure 13. Relations among gas utilization factor and electron production cost at 0.15 mg/s of mass flow rate and 40V of anode voltage.

V. Conclusion

Through the experimental evaluations of ignition capability and electron emission performance at the inductively coupled plasma cathode, the following results have been obtained,

1. The ignition capability of ICP/C is influenced by inner pressure and electric field in the vessel strongly. Thus, the pressure rise by changing orifice dimensions and the voltage rise by increase of the total number of coils cause the enhancement of ignition capability.
2. The electron emission performance depends on the ion saturation current at the ion sheath formed on the ion collector. Additionally, the performance was affected by inner pressure, ion collection area, electron number density and total number of coils.
3. The gas utilization factor increases as RF power increase at constant electron production cost.
4. When the pole collector is inserted into the cathode, the typical electron emission performance was 0.52 A of the anode current at 24 W of RF power, 0.15 mg/s of Xe mass flow rate and 40 V of anode voltage. The values of current is high enough to neutralize ion beam of ion thrusters, which have been employed for north south station keeping missions.

Acknowledgments

The Authors would like to express their sincere thanks to Dr. Kuriki, K. (Professor Emeritus, Institute of Space and Astronautical Science) for helpful discussions and technical supports. This study was supported by a Grant-in-Aid for Young Scientists (B), No. 22760625, sponsored by Japan society for the promotion of science.

References

[1]Dan M, Gebbel and Ira Katz, *Fundamentals of Electric Propulsion: Ion and Hall Thruster*, JPL Space Science and Technology Series, John Wiley & Sons, 2008, Chap. 9.

[2]Ioannis G. Mikellides and Ira Katz, "Wear Mechanisms in Electron Sources for Ion Propulsion, 1: Neutralizer Hollow Cathode," *Journal of Propulsion and Power*, Vol. 24, No. 4, 2008, pp. 855-865.

[3]Ioannis G. Mikellides, Ira Katz, Dan M. Goebel, Kristina K. Jameson and James E. Polk, "Wear Mechanisms in Electron Sources for Ion Propulsion, 2: Discharge Hollow Cathode," *Journal of Propulsion and Power*, Vol. 24, No. 4 2008, pp. 866-879.

[4]Yevgeny Raitses, Jennifer K. Hendryx and Nathaniel J. Fisch, "A Parametric Study of Electron Extraction from a Low Frequency Inductively Coupled RF-Plasma Source," 31st International Electric Propulsion Conference, IEPC-2009-024, 2009.

[5]John E. Foster and Michael J. Patterson, "Discharge Characterization of 40-Centimeter Microwave Electron Cyclotron Resonance Ion Source and Neutralizer," *Journal of Propulsion and Power*, Vol. 21, No. 5, 2005, pp. 862-869.

[6]Ikkoh Funaki and Hitoshi Kuninaka, "Overdense Plasma Production in a Low-power Microwave Discharge Electron Sourse," *Japanese Journal of Applied Physics*, Vol. 40, Part. 1, No. 4A, 2001, pp. 2495-2500.

[7]Ben Longmier and Noah Hershkowitz, "Improved operation of the nonambipolar electron source," *Review of Scientific Instuments*, Vol. 79, Issue 9, 2008, 093506.
[8]Hitoshi Kuninaka, Kazutaka Nishiyama, Yukio Shimizu, Ikkoh Funaki, Hiroyuki Koizumi, Satoshi Hosoda and Daisuke Nakata, "Hayabusa Asteroid Explorer Powered by Ion Engines on the way to Earth," 31st International Electric Propulsion Conference, IEPC-2009-267, 2009.
[9]Hiroki Watanabe, Takuji Okuma, Junichiro Aoyagi and Haruki Takegahara, "Research and Development on Inductively Coupled Plasma for Ion Engines," 31st International Electric Propulsion Conference, IEPC-2009-027, Michigan, USA, 2009.
[10]Hideo Sugai,, Kenji Nakamura and Keiji Suzuki, "Electrostatic Coupling of Antenna and the Shielding Effect in Inductive RF plasma," *Japanese Journal of Applied Pysics*, Vol. 3, Part1, No. 4B, 1994, pp. 2189-2193
[11]Richard H. Huddlestone and Sanley L. Leonard, *Plasma Diagnostic Thechniques*, Academic Press, 1965, Chap. 4.
[12]Ahmad Nazri Dagang, Akira Kondo, Hideki Motomura and Masafumi Jinno, "Mercury-free electrodeless discharge lamp; effect of xenon pressure and plasma parameters on luminance," *Journal of physics D: Applied Physics*, Vol. 42, Issue 9, 2009, 095202.
[13]R. M. Castro, G. A. Cirino, P. Verdonck, H. S. Maciel, M. Massi, M. B. Pisani and R. D. Mansano, "A Comparative Study of Single and Double Langmuir Probe Techniques for RF Plasma Characterization," *Contributions to Plasma Physics*, Vol. 39, Issue 3, 1999, pp. 235-246.
[14]Tetuo Fujimoto and Masaru Usami, "Rarefied Gas Flow Through a Circular Orifice and Short Tubes," Transactions of the ASME, *Journal of Fluids Engineering*, Vol. 106, 1984, pp. 367-373.
[15]S. Varoutis, D. Valougeorgis, O. Sazhin and F. Sharipov, "Rarefied gas flow through short tubes into vacuum," *Journal of vacuum and Technology A: Vacuum, Surfaces, and Films*, Vol. 26, Issue 2, 2008, pp. 228-238.
[16]A. D. Macdonald and Sanborn C. Brown, "High Frequency Gas Discharge Breakdown in Helium," Physical Review, Vol.75, No. 3, 1949, pp. 411-418.
[17]Kenichi Kajiwara, Masafumi Ikeda, Hiroki Kohata and Toshiyuki Ozaki, "ETS-Ⅷ Ion Engine and its Operation on Orbit," 31st International Electric Propulsion Conference, IEPC-2009-048, 2009.
[18]Noah Hershkowitz, "Sheaths: More complicated than you think," *Physics of Plasmas*, Vol. 12, Issue 5, 2005, 055502
[19]R. B. Picjak, V. A. Godyak and B. M. Alexandrovich, "A simple analysis of an inductive RF discharge," *Plasma Sources Science and Technology*, Vol. 1, No. 3, 1992, pp. 179-186.
[20]J. Hopwood, "Planar RF induction plasma coupling efficiency," *Plasma Sources Science and Technology*, Vol. 3, No. 4, 1994, pp. 460-464.